Hydrodynamic and Topological Interactions in Sedimentation of Poly(methyl methacrylate) in Semidilute Solutions of Polystyrene in Thiophenol†

Norio Nemoto,* Shinichi Okada, Tadashi Inoue, and Michio Kurata

Institute for Chemical Research, Kyoto University, Uji, Kyoto-fu 611, Japan.
Received July 23, 1987; Revised Manuscript Received November 12, 1987

ABSTRACT: This work has been performed to clarify effects of two dynamical interactions, the hydrodynamic interaction and the topological interaction, on transport of a flexible chain molecule in the semidilute regime. The sedimentation velocity technique has been applied to obtain the sedimentation coefficient s of poly(methyl methacrylate) over a range of molecular weight (MW) from 107 000 to 4 050 000 in semidilute solutions of polystyrene with three different MWs (M_{PS} = 43 900, 775 000, and 8 420 000) in thiophenol. The steady viscosity of PS solutions with M_{PS} = 43 900 and 775 000 has been also measured. In semidilute solutions of PS with M_{PS} = 43 900 in which the topological interaction is negligible, MW dependence of s could be described by the dilute solution theory for the nondraining chain with a finite number of segments. For analysis of s data in solutions of PS with M_{PS} = 8 420 000, the Rouse model of n segments with effective friction coefficient $\zeta(c_{PS})$ has been used. The effect of the hydrodynamic screening has been found as $\zeta(c_{PS}) \propto c_{PS}^{0.68\pm0.02}$. The effect of the topological interaction has been manifested on a master curve constructed, by use of the MW between entanglements, $M_{e,PS}$, from the s data after subtraction of the hydrodynamic screening effect. In solutions of PS with M_{PS} = 775 000, it has been found that a different transport mechanism may become dominant depending on both a ratio of M to M_{PS} and PS concentration. Concerning the concentration dependence, all reduced plots of s/s_0 versus c_{PS} could be superposed on the reduced viscosity curve.

Introduction

In the semidilute regime, two dynamical interactions, the *topological interaction* as well as the *hydrodynamic interaction*, affect the Brownian motion of a flexible chain molecule. Here the semidilute regime is defined as the regime where chains overlap one another, but polymer concentration c is as yet so low that the local segmental motion is not perturbed by other chain segments. This means that the friction constant ζ of a segment with a radius a can be written as $\zeta = 6\pi\eta_0 a$ by using solvent viscosity η_0. The excluded-volume effect still persists in this regime but becomes less important with increasing c in comparison with the dynamical effects. The scaling theory combined with the tube model has elegantly explained effects of the two interactions on the self-diffusion behavior of a polymer in highly entangled solutions.[1] Pioneering FRS measurements[2] on semidilute solutions of polystyrene (PS) in benzene confirmed the theoretical prediction of $D_s \propto M^{-2}c^{-1.75}$ in a good solvent. However, later studies showed that the above relation concerning c dependence held only in a limited range of concentration.[3,4] Quite recently, Wheeler et al.[5] have shown that the tracer diffusion coefficient D_{tr} of PS in solutions of poly(vinyl methyl ether) (PVME) in *o*-fluorotoluene is proportional to $M^{-\beta}$ at all concentrations studied and that the exponent β gradually increases with increasing c_{PVME} from 0.55 in pure *o*-fluorotoluene to 1.89 at the highest concentration of 0.1 g cm^{-3} investigated where PVME chains are entangled. There has been no symptom for the exponent β to approach asymptotically to the theoretical value of 2 at higher c_{PVME}. The increase in β with increasing c has been also noticed by Callaghan and Pinder.[4] The presence of such a broad transition region from the Zimm behavior to the reptation behavior is not unexpected if we accept that above the critical overlapping concentration c^*, there exists a concentration regime where polymer chains extensively overlap but are not yet entangled, in referring to viscoelastic data. In this concentration regime where the tube is not formed, therefore, it seems to be meaningless to discuss the diffusion behavior based on the tube model[1,6] or its modification like the tube renewal or constraint release.[7,8] Furthermore we should pay more attention to the influence of the hydrodynamic interaction on the molecular weight dependence of D_s. For homogeneous solutions of polymers with uniform molecular weight, the hydrodynamic interaction must be fully taken into account at c^* where polymer chains just start to contact one another, and it is going to be gradually screened with increasing c. This would give rise to a transition from Zimm behavior of $D_s \propto M^{-\nu}$ (ν = 0.5–0.6) to Rouse behavior of $D_s \propto M^{-1}$ without the topological interaction. Since the topological interaction may also start to affect the dynamics above c^*, the increase in the exponent β with increasing c is a combined effect of the two interactions on the slow diffusion motion. Separation of the two effects looks to be quite difficult for homogeneous solutions.

One characteristic feature of the hydrodynamic interaction effect in the semidilute regime may be revealed by making measurements of D_{tr} of a polymer whose molecular weight M_N is much larger than M_P of a host polymer molecule. In this case, the conformational longest relaxation time of the host P chain is much shorter than the corresponding time of the tracer N chain, and also the P chain diffuses much faster than the N chain if P chains are not entangled. The finite coil size of the P chain may be only effective in the determination of the size of the block between which full hydrodynamic interaction should be taken into account. The topological interaction between the N and the P chains can be absorbed into the friction constant of the block. Then the host polymer solution may be regarded as a viscous solvent to the slow motion such as the self-diffusion of the N chain. In analogy to the translational diffusion in the dilute regime, the dependence of D_s on M may be close to the nondraining Zimm case and also dependence of the reciprocal proportionality of D_s on the solution viscosity η is expected. The similar conjecture might be also valid for diffusion in entangled solutions of P chains as long as the longest relaxation time of the P chain matrix is shorter than the characteristic time for the self-diffusion of the N chain. This case has been studied by Nose and his co-workers in detail.[9]

The case of $M_N \ll M_P$ gives an opportunity to study the screened hydrodynamic interaction. The model to be adopted is the Rouse chain consisting of n segments with

† Part 4 of a series of "Dynamics of Polymer–Polymer–Solvent Ternary Systems".

0024-9297/88/2221-1502$01.50/0 © 1988 American Chemical Society

Table I
Characterization of PMMA and PS

sample code	$M_W \times 10^{-4}$	s_0, 10^{-13} s	k_s, cm^3 g^{-1}
PMMA			
P-4	10.7	1.15	87
P-1[a]	26.0	1.63	126
P-5	26.5	1.66	150
P-6	40.1	2.08	201
P-7	84.4	2.56 ± 0.12	315 ± 30
80M	110	3.06 ± 0.07	375 ± 30
75M	214	3.94 ± 0.13	615 ± 40
P-400	405	4.88 ± 0.12	955 ± 70

[a] The sample used in ref 16 and 17.

effective friction coefficient $\zeta(c)$. Theories predict that $\zeta(c)$ is not dependent on either M_N or M_P but dependent only on c as $\zeta \propto c^\gamma$ with $\gamma = 0.5$ in the good-solvent limit and 1 in the Θ-state.[10,11,27,28] Then the deviation of molecular weight dependence of D_s from $D_s \propto M^{-1}$ is directly related to the effect of the topological interaction between the tracer polymer and the surrounding matrix polymers. Since the concentration dependence of ζ can be estimated from D_s data of the low molecular weight polymer to which the topological interaction is negligible, the effect of the topological interaction on the dependence of D_s on concentration as well as molecular weight can be elucidated from higher MW data corrected for the hydrodynamic screening effect. In a recent study of Kim et al.,[12] D_{tr}^{∞}, a limiting asymptotic value of D_{tr}, independent of M_P, has been derived over a wide range of c and M_N for PS solutions and has been analyzed with the same spirit as mentioned above. The hydrodynamic screening effect on D_{tr}^{∞} has been considered on the basis of the blob model. They have found that, at the high ends of M_N and c, $D_{tr}^{\infty} \propto M_N^{-3}c^{-3}$ is a better representation of the data than the theoretical relation $D_{tr}^{\infty} \propto M^{-2}c^{-1.75}$. The disagreement between their results and earlier experimental results suggests that the situation is quite complicated and that more careful and accurate experimental studies should be conducted.

In parts 1[13] and 2[14] of this series on the "Dynamics of Polymer–Polymer–Solvent Ternary Systems", we have shown that the sedimentation coefficient s of a tracer poly(methyl methacrylate) (PMMA) can be accurately measured in semidilute solutions of a isopycnic pair of PS and thiophenol and also that s data give quite the same information on a friction coefficient of a molecule in the semidilute regime as D_s data do. In this paper, the s of PMMA has been measured in the wide range of M from 107 000 to 4 050 000 in semidilute solutions of PS with three different MWs of 43 900, 775 000, and 8 420 000. The steady viscosity of the PS solutions with the two lower MWs has also been measured. New methods for data analysis have been proposed and shown to be quite effective for a study of effects of the hydrodynamic and the topological interactions on a friction coefficient of a flexible polymer molecule in the semidilute regime.

Experimental Section

Materials. Seven samples of poly(methyl methacrylate) with different MW have been used in this study. Four PMMA samples (sample code P-4, -5, -6, and -7), having a MW in the range $107\,000 \le M \le 844\,000$, were purchased from Polymer Laboratories Ltd. One sample with the highest MW (P-400; a gift from Prof. Nose of Tokyo Institute of Technology) was obtained by the radical polymerization method and subsequent fractionation.[9] The remaining two samples (80M, 75M) are gifts from Dr. Fukuda of this institute and have been characterized by him and his coworkers.[15] These PMMA samples were purified by dissolving them in benzene and precipitating in methanol. Their molecular weights are listed in Table I where the MW of the sample P-1 used in part 2 is also included.[16] Three narrow-distribution molecular weight polystyrene samples (M_w = 43 900 (sample code F4), 775 000 (F80), and 8 420 000 (F840), Toyo Soda) were used as a host polymer of the polymer–polymer–solvent ternary systems without further purification. Reagent-grade thiophenol (TPh, Nakarai Co.) was purified and stored as described elsewhere.[14]

Table II
Characteristics of PS Solutions Used as a Matrix Solution

PS	$M_W \times 10^{-4}$	c_{PS}, 10^{-2} g g^{-1}	c^*_{PS}, 10^{2} g g^{-1}	$c_{e,PS}$, 10^{-2} g g^{-1}
F4	4.39	5–22	3.59	37.5
F80	77.5	1–16	0.482	4.8
F840	842	0.5–5	0.0907	0.88

It has been found in part 1[13] based on dynamic light scattering measurements on the sample P-1 that thiophenol is a good solvent for PMMA. This was reconfirmed by measuring the sedimentation coefficient s of PMMA in TPh in the dilute regime. By fitting eq 1 to the s data, we obtained the sedimentation coefficient at infinite dilution, s_0, and the concentration coefficient k_s.

$$1/s = (1/s_0)(1 + k_s c) \quad (1)$$

The values of s_0 and k_s obtained are given in Table I.[17] MW dependence of s_0 and k_s can be expressed by eq 2 and 3, respectively. The exponent 0.4 in eq 2 indicates that TPh is a good solvent for PMMA.[18] TPh was shown, in part 1, to also be a good solvent for PS, to the same extent as benzene is.

$$s_0 = 1.17 \times 10^{-13} M^{0.40\pm0.02} \quad \text{(s)} \quad (2)$$

$$k_s = 2.5 \times 10^{-2} M_w^{0.69\pm0.02} \quad (\text{g}^{-1}\ \text{cm}^3) \quad (3)$$

Ternary solutions were prepared by dissolving PMMA and PS in the purified TPh and stirring for a week when the steady viscosity η of these solutions was lower than about 1 poise. When $\eta > 1$ P, the polymers and the solvent were put into a small glass tube, and the tube was sealed under nitrogen atmosphere. The sealed tube was put in an electric oven thermostated at ca. 50 °C and was rotated in a tilted state with 2 revolutions per hour for at least 2 months. The sedimentation coefficient s has been reproducible for solutions with prolonged periods of preparation, indicating that the solutions thus prepared are homogeneous. Concentrations of solutions were determined by weighing. PMMA concentration was fixed at 0.1 wt % for samples with $M \le 844\,000$ and lowered to 0.03–0.04 wt % for higher MW samples. Concentration ranges of PS investigated for respective series (F4, F80, and F840 series) are given in Table II. Values of the so-called critical overlapping concentration c^*_{PS} estimated earlier[14] are listed in the fourth column of Table II. It is seen that all solutions investigated belong to the semidilute regime. Values of the critical entanglement concentration $c_{e,PS}$ were also estimated[19] and are given in the fifth column of Table II.

Methods. Sedimentation velocity experiments on the ternary systems were performed at 25 ± 0.05 °C by using an analytical ultracentrifuge (Beckman Spinco Model E). The rotor speed was 59 780 rpm. A single peak due to the sedimentation of PMMA molecules has been observed in photographs of the sedimentation pattern. Therefore the sedimentation coefficient s has been estimated by the standard procedure to an accuracy of 5%. The s was found to be independent of the rotor speed.

Steady viscosity of PS solutions of F4 and F80 series has been measured with either an Ubelohde or an Ostwald type of viscometer at 25 ± 0.1 °C.

Results and Discussion

1. Sedimentation Behavior in Low MW PS Solutions (F4 Series); $M > M_{PS}$. Figure 1 shows molecular weight dependence of s of PMMA in TPh solutions of PS with M_{PS} = 43 900 at c_{PS} = 16.8 and 22.0 wt %. Infinite dilution s_0 data in pure TPh are also shown for comparison. In the high MW region, s at both c_{PS} appears to increase with increasing M with about the same exponent of 0.4 as s_0 does. At the low MW end, however, the curves slightly deviate from $s \propto M^{0.4}$. Since PS and TPh are isopycnic with each other and also the concentration of PMMA is

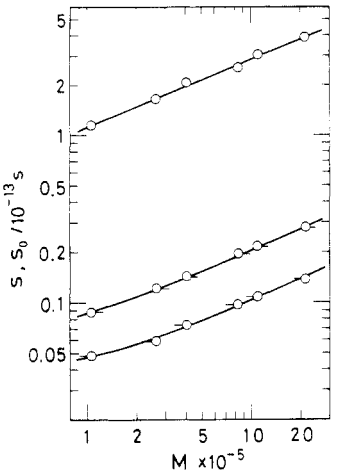

Figure 1. Molecular weight dependence of the sedimentation coefficient s of PMMA in thiophenol and in solutions of PS (M_w = 43 900) in thiophenol. Symbols: (○) s at infinite dilution of PMMA in thiophenol; (⊖) in the PS solution of c_{PS} = 16.8 wt %; (⊖) in the PS solution of c_{PS} = 22.0 wt %. The solid line to s_0 data at the top is eq 2. The lower curves to s data have been calculated by using eq 9 with h^* = 0.27 and 0.21 for c_{PS} = 16.8 and 22.0 wt %, respectively.

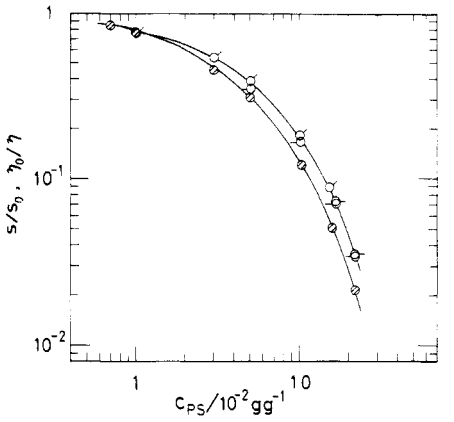

Figure 2. Comparison of the two reduced quantities, η_0/η and s/s_0 for the F4 series. Symbols are (⊘) the reciprocal of the reduced steady viscosity of host PS solutions (M_W = 43 900) and (○) the reduced sedimentation coefficient of PMMA in corresponding PS solution. M_{PMMA} = 260K (⊘); 1100K (⊖); 2140K (⊖).

as low as 0.1 wt %, s can be directly related to the friction coefficient f of a PMMA molecule in semidilute solutions of PS in TPh by eq 4 as in dilute homogeneous polymer

$$s = \frac{M}{N_a f}(1 - \bar{v}\rho) \tag{4}$$

solution. Here N_a is the Avogadro constant, $\bar{v}$ the specific volume of PMMA and, ρ the density of the solution. f is related to the self-diffusion coefficient D_s as

$$f = RT/N_a D_s \tag{5}$$

It is well-known that, in pure thiophenol, the friction coefficient at infinite dilution of PMMA, f_0, can be used to define the hydrodynamic radius of the polymer R_H^0 as eq 6 from application of the Stokes law for hydrodynamic friction of a rigid spherical particle in low molecular liquid.

$$f_0 = 6\pi\eta_0 R_H^0 \tag{6}$$

where η_0 is the viscosity of the solvent. When M is much larger than M_{PS} in the ternary systems, it might be assumed that a PMMA molecule sediments as an impermeable sphere with a radius R_H through continum liquid with the solution viscosity η. Then f of PMMA in the solutions can be written similarly as

$$f = 6\pi\eta R_H \tag{7}$$

From eq 4, 6, and 7,

$$s/s_0 = f_0/f = (\eta_0/\eta)(R_H^0/R_H) \tag{8}$$

Figure 2 shows comparison between s/s_0 and η_0/η, which are logarithmically plotted against c_{PS}. η_0 is measured as $1.144 \times 10^{-2}\ p$ at 25 ± 0.1 °C. Curves drawn empirically in the figure clearly show that dependences of the two reduced quantities on c_{PS} become stronger with increasing c_{PS}. Above c_{PS}^* (=3.59 wt %), s/s_0 is always larger than η_0/η and the ratio of s/s_0 to η_0/η appears to take a constant value of about 1.6 at higher c_{PS}. The difference might be attributed to the shrinkage of the polymer coil, since TPh is a good solvent for PMMA whereas a mixture of PS and TPh, a polymer–solvent, is surely a poor solvent.[29] However, if the polymer dimension were close to that of the unperturbed state in the solutions at higher c_{PS} and the hydrodynamic interaction between PMMA segments were fully effective, s should increase as $s \propto M/f \propto M^{0.5}$ with increase in M, and also s/s_0 should depend on M due to the MW dependence of R_H^0/R_H. As is clear from Figures 1 and 2, these expectations are not in agreement with experimental findings. In order to solve this contradiction, let us assume that the weaker MW dependence of s at the low MW end is attributed to that M of PMMA becomes comparable with M of the medium PS in this low MW region. The effect of the finite coil size of PS chains on the hydrodynamic interaction between PMMA segments is quite complicated but may be crudely taken into account by assuming that a PMMA chain is in the unperturbed state and it consists of N (=M/M_{PS}) blocks whose friction coefficient is f_B and between which the hydrodynamic interaction is fully taken into account. Since M_{PS} is low, it seems to be reasonable to suppose that the effect of the topological interaction on f is negligible or it affects the magnitude of f_B a little bit. Then the Kirkwood–Riseman formalism for dynamics of an isolated chain[20] is applicable for analysis of the data in Figure 1.

$$\frac{1}{f} = \left(\frac{1}{Nf_B}\right)\left(1 + \frac{8}{3}2^{1/2}h^*N^{1/2}\right), \quad N > 1 \tag{9}$$

Here h^* is a draining parameter, and h^* = 0 corresponds to no hydrodynamic interaction and h^* = 0.27 to the dominant hydrodynamic interaction case.[21] In a fit of eq 9 to the s data, f_B may be treated as an adjustable parameter while the h^* value is fixed at 0.27. By taking into account the rough definition of N being assumed to be independent of PS concentration, however, both h^* and f_B have been treated as adjustable parameters in the following fitting procedure. That is, h^* has been determined as a value with which eq 9 most closely represents the observed increase of s with increasing M, while f_B is adjusted so as to get coincidence between the calculated and the experimental value of s at M = 107 000. Theoretical curves calculated are shown as solid curves with h^* = 0.27 for c_{PS} = 16.8 and h^* = 0.21 for c_{PS} = 22.0 wt %. It should be noted that the use of h^* = 0.27 for a fit of eq 9 to the latter solution data is allowable to an experimental accuracy. The good reproducibility of the MW dependence of s by those curves indicates that the effect of the hydrodynamic interaction on sedimentation of PMMA in unentangled PS solutions with $M_{PS} < M$ has been properly explained by the present simple model.

2. Sedimentation Behavior in Intermediate MW PS Solutions (F80 Series); $M \geq$ and $\leq M_{PS}$.

Table III
Sedimentation Coefficient s of PMMA in PS–TPh Solutions in Units of 10^{-13} s

PS	c_{PS}, wt %	P-4	P-1[a]	P-5	P-6	P-7	80M	75M	P-400
F4	1		1.22						
	3		0.88						
	5		0.64					1.37	
	10		0.30					0.66	
	16.8	0.89	0.145	0.121	0.142	0.195	0.22	0.28	
	22	0.48		0.59	0.074	0.096	0.108	0.137	
F80	1	0.78	0.76	0.74	0.77	0.87	0.94	1.07	
	3	0.4	0.30	0.31	0.26	0.25	0.26	0.26	
	5	0.21	0.16	0.169	0.149	0.110	0.104	0.099	
	10	0.075		0.046	0.034	0.020	0.0163		
	16	0.029	0.0113	0.0118	0.0082				
F850	0.5	0.77	0.91	0.89	0.91	0.99	0.96	0.91	0.87
	1	0.60	0.62	0.65	0.66	0.58	0.50	0.43	0.34
	2	0.41	0.38	0.40	0.35	0.28	0.21	0.138	0.083
	3.8	0.26	0.183	0.197	0.158	0.098	0.067	0.034	0.0179
	5	0.186		0.131	0.098	0.051	0.037	0.0176	0.0091

[a] From Table III in ref 17.

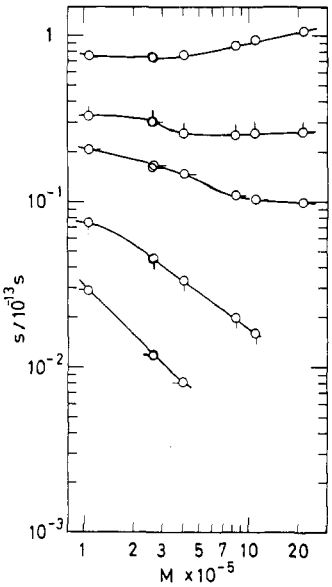

Figure 3. Molecular weight dependence of the sedimentation coefficient s of PMMA in solutions of PS (M_W = 775 000) in thiophenol. PS concentration is, from the top, 1.0 (○), 3.0 (◑), 5.0 (◒), 10.0 (◔), and 16.0 wt % (●), respectively.

2.1. Molecular Weight Dependence of s. Figure 3 shows molecular weight dependence on s of PMMA in semidilute solutions of PS with M_{PS} = 775 000 in the range of c_{PS} from 1 to 16 wt %. It has turned out that the curves, obtained by simply connecting respective data points, change their slopes from a positive to a negative sign with increasing c_{PS}. The whole aspect may be qualitatively interpreted as that at lower c_{PS}, the hydrodynamic interaction dominates the behavior, and in the range of c_{PS} higher than $c_{e,PS}$ (=4.8 wt %) the effect of the topological interaction becomes dominant. Here $c_{e,PS}$ has been estimated by using an empirical equation reported in ref 19. At c_{PS} = 1 wt %, s is independent of M up to $M \leq$ 401 000 and then increases gradually with increasing M. At this concentration, PS chains overlap one another, but their respective translational diffusion motion is only slightly affected by other chains, owing to a large amount of solvent. As long as M of the diffusing PMMA molecule is much smaller than that of the PS molecule, therefore, the screening effect of the hydrodynamic interaction by PS chains may lead to the free-draining behavior of $f \propto M^1$ for PMMA. For $M > M_{PS}$, the hydrodynamic interaction is partially screened, which gives rise to the gradual increase of s with M, or $f \propto M^{\nu'}$ ($0.5 < \nu' < 1$). This case has been already encountered for the F4 series in the previous section. At c_{PS} = 3 wt %, the s changes by only 30% during the 20-fold change of M of PMMA. The approximate free draining behavior of $f \propto M^1$ over the entire range of M studied may come from a cancellation of two effects of the topological and the hydrodynamic interaction, because the former tends to make MW dependence of f stronger than $f \propto M^1$ at low M, and the latter acts in the opposite direction at higher M.

At c_{PS} = 5 wt % close to $c_{e,PS}$, s decreases with increasing M due to the topological interaction to the extent that s at M = 844 000 becomes one-half of s at M = 107 000. Above M = 844 000, s becomes almost independent of M. The latter behavior indicates that the topological interaction becomes less effective whenever the characteristic time for diffusion of PMMA becomes comparable with the longest relaxation time associated with the overlapped PS chains. In this connection, we should notice the finding of Nose and his co-workers[9] that the tracer diffusion coefficient $D_{tr,PS}$ of high MW PS in highly entangled PMMA solutions obeys the generalized Einstein–Stokes relation when M of the diffusing PS molecule is much higher than that of a matrix PMMA. That is, the entanglement effect due to the PMMA matrix is absorbed into the increase of the solution viscosity and does not affect the MW dependence of $D_{tr,PS}$. Simple application of their arguments leads us to an expectation that at much higher M, s again increases with M as $s \propto M^{0.5}$.

With further increase in c_{PS} above 5 wt %, the entanglement network formed by PS chains greatly hinders the translational motion of a PMMA chain. Thus s not only drastically decreases in absolute magnitude but also exhibits stronger MW dependence at higher c_{PS}. At c_{PS} = 16 wt %, s is proportional to M^{-1}, which is in agreement with the prediction of the reptation model of $D_s \propto M^{-2}$.[22]

The gradual increase in the MW dependence of s observed for $M < M_{PS}$ with increasing c_{PS} is qualitatively in agreement with results of Wheeler et al. described in the introduction.[5] The presence of a broad c_{PS} region for transition from $f \propto M^1$ to $f \propto M^2$ behavior indicates that overlapping of polymer chains is a condition necessary for the topological interaction to become effective on polymer diffusion. Immobilization of chains surrounding the diffusing molecule seems to be more important for the reptation motion, otherwise lateral and parallel diffusional motion along the chain axis are both significant. Indeed, a sphere model with or without the hydrodynamic inter-

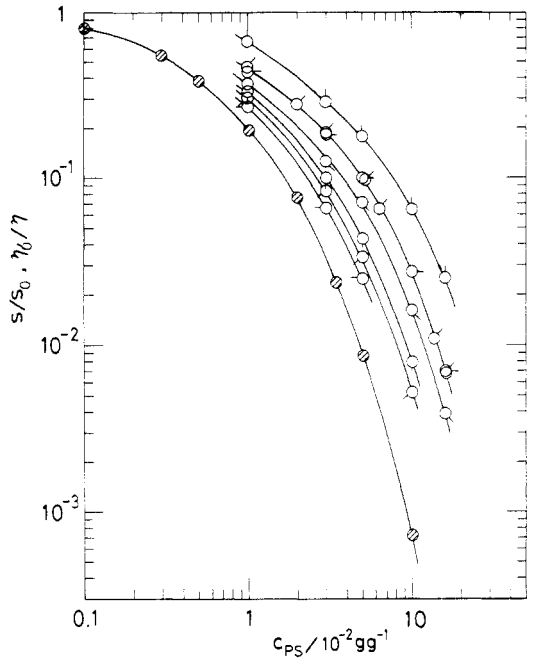

Figure 4. Dependence of s/s_0 and η_0/η on PS concentration for the F80 series. Symbols are (○) s/s_0 and (⊘) η_0/η. Molecular weight of PMMA is 107K (◔); 260K (◑); 265K (◕); 401K (●); 844K (◒); 1100K (◒); and 2140K (◒).

action seems to be a better model for $M > M_{PS}$.

2.2. Concentration Dependence of s. In part 2,[14] we have reported that dependence of s of PMMA on PS concentration can be represented by eq 10. Its validity

$$s/s_0 = \exp(-Ac^{\delta}) \qquad (10)$$

for various polymer–solvent systems has been recently discussed in detail by Phillies.[23] The s/s_0 data for each molecular weight of PMMA in Figure 4 have been fitted quite well to eq 10, as is shown by the solid curves. δ was found to take a constant value of 0.62 ± 0.01 for $M \geq$ 401 000. This value is in accord with values obtained for rigid spheres in polymer solutions from either dynamic light scattering or sedimentation velocity measurements. A slightly larger value of δ = 0.65 was found for M = 107 000 and 265 000. The variation in δ with M of PMMA is quite small compared with the corresponding change in δ with M of PS. For example, δ was found as 0.80 for s data of the F4 series. On the other hand, generalization of eq 10 to include MW dependence of s, i.e., by writing $A = A'M^{\mu}$, has failed. For s of flexible polymers, thus, the exponential type of equation such as eq 10 seems to be a useful functional form only for representation of its concentration dependence.

Figure 4 also shows the concentration dependence on η of PS matrix solutions in the reciprocal reduced form. s/s_0 is always larger than η_0/η. The ratio of s/s_0 to η_0/η is about 3 at the highest M of 2 140 000. At first glance we expect that all s/s_0 versus c_{PS} curves can be superposed on the η_0/η curve by horizontal shifting alone. Results of superposition are shown in Figure 5, and the shift factor a_M used is plotted against M of PMMA in Figure 6. Here the curve has been drawn by connecting data points. A similar superposition procedure has been also attempted for η and s data of the F4 series, and results are shown in Figures 5 and 6. Obviously, excellent superposition has been accomplished for the both series. The MW dependence of this shift factor is, however, quite different. For the F4 series, a_M is small and independent of M, indicating that the transport of a PMMA molecule can be described by use of the macroscopic viscosity. For the F80 series,

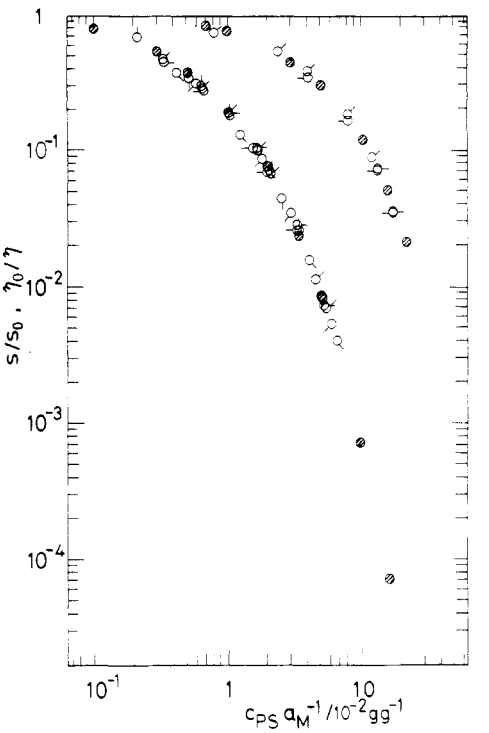

Figure 5. Superposition of s/s_0 on η_0/η for the F4 and F80 series. The upper curve is for F4 series and the lower one for the F80 series. Symbols are the same as in Figures 2 and 4, respectively.

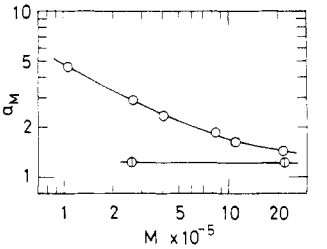

Figure 6. Shift factor a_M obtained from the superposition in Figure 5. Symbols are (○) F80 series and (◔) F4 series.

on the other hand, a_M is approximately proportional to $M^{-0.5}$ in the range of $M < M_{PS}$ and becomes less dependent on M for $M > M_{PS}$. Since c^*_{PS} is proportional to $M^{-0.7}$,[14] $c_{PS}a_M$ is not proportional to c_{PS}/c^*_{PS}. Thus it may be concluded that s/s_0 cannot be scaled by c_{PS}/c^*_{PS} even for $M < M_{PS}$. At present we do not have any explanation why superposition of s/s_0 to η_0/η is so successful. It might be apparent or might have more profound physical significance. Any way, our view is simply summarized as that examination of MW dependence of s gives a deeper insight into the transport mechanism of a tracer polymer in the semidilute solutions of another matrix polymer than examination of c dependence on s.

3. Sedimentation Behavior in High MW PS Solutions (F840 Series); $M < M_{PS}$. Figure 7 gives dependence of s on molecular weight of PMMA in semidilute solutions of PS with M_{PS} = 8 420 000 in the range of c_{PS} from 0.5 to 5 wt %. The molecular weight of M_{PS} = 8 420 000 has been chosen with the expectation that we shall be able to study a limiting case of the sedimentation of a tracer polymer through a spatially fixed polymer network. In other words, it has been desired that s of a tracer (M_N) no longer depends on molecular weight of a matrix polymer (M_P) but on a quantity characteristic of the entanglement network, for example, the molecular weight between entanglements M_e. Although dependence of s on M_{PS} has not been examined in a higher M_{PS} region, we would like to refer to

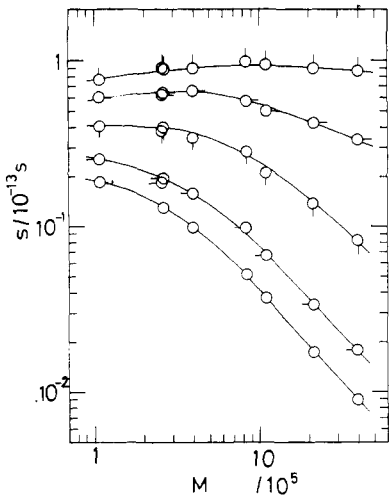

Figure 7. Molecular weight dependence of the sedimentation coefficient s of PMMA in solutions of PS (M_W = 8 420 000) in thiophenol. PS concentration is, from the top, 0.5 (◇), 1.0 (○), 2.0 (○), 3.8 (○), and 5.0 wt % (○). The solid curve for each concentration has been used to estimate a value of $s(0.1M_{e,PS})$ empirically at each concentration by either interpolation or extrapolation.

results reported by two groups. Kim et al.[12] have shown that D_{tr} of PS becomes independent of the matrix molecular weight of M_P when M_P becomes larger than the molecular weight of the tracer polymer M_N by a factor of 3–5. Marmonier and Leger have reached a similar conclusion.[24] Six PMMA samples with M from 107 000 to 2 140 000 approximately satisfy this criterion but the sample P-400 with M = 4 050 000 does not. Thus it should be kept in mind that s values of the former six samples given in Table III may be very close to values to be derived in solutions of PS with infinite molecular weight, whereas values of P-400 are a little bit larger.

Since the hydrodynamic interaction between PMMA segments is screened by overlapping PS chains, the PMMA chain may be substituted for the free-draining Rouse chain of n segments with effective friction coefficient ζ which depends only on c_{PS}. Strong MW dependence of s observed at higher c_{PS} and M in Figure 7 is due to the topological interaction between PMMA and the surrounding PS matrix. When we express this effect on f by a topological function ψ, f is given as

$$f = n\zeta\psi \tag{11}$$

In general, ψ is a function of M, M_{PS}, and c_{PS}. In a limit of $M_{PS} \to \infty$, PS chains form a spatially fixed entanglement network which is characterized by $M_{e,PS}$. Substituting eq 11 into eq 4, we obtain

$$s = K/\zeta(c_{ps})\psi\ (M/M_{e,PS}) \tag{12}$$

Here K is a constant. In order to calculate ψ from s, $\zeta(c_{PS})$ in eq 12 must be known. $\zeta(c_{PS})$ can be estimated by the following method. When the molecular weight of a diffusing PMMA molecule is much smaller than the mesh size of the network $M_{e,PS}$, ψ in eq 12 can be taken as unity for s of the sample with that particular molecular weight. For this purpose we here take $M = 0.1M_{e,PS}$ at which ψ may be close to unity. $M_{e,PS}$ was estimated by using an empirical relation obtained from viscoelastic measurements on semidilute solutions of high MW PS in aroclor.[19,30]

$$c_{PS}^{1.4}M_{e,PS} = 1.23 \times 10^4 \quad (g/cm^3)^{1.4} \tag{13}$$

A value of s at $M = 0.1M_{e,PS}$, $s(0.1M_{e,PS})$, can be easily read from respective s versus M curves in Figure 7 by interpolation to the data for $c_{PS} \leq 3.8$ wt % and by extrapolation to the data at c_{PS} = 5 wt %. $\zeta(c_{PS})$ is related to $s(0.1M_{e,PS})$ by eq 14. The topological function ψ now can

$$s(0.1M_{e,PS}) = K/\zeta(c_{PS}) \tag{14}$$

be readily calculated from eq 12 and 13 as

$$s/s(0.1M_{e,PS}) = 1/\psi(M/M_{e,PS}) \tag{15}$$

Equation 15 indicates that when the variables s and M in Figure 7 are reduced by $s(0.1M_{e,PS})$ and $M_{e,PS}$, respectively, all data points may form a single composite curve. The results are shown in Figure 8. It is remarkable that all data (unfilled circles) are located on a master curve within an experimental uncertainty of 5% except a few points belonging to the sample P-400. It was already noted that s values obtained for this highest MW PMMA may be larger, because of $M_{PS}/M \simeq 2$, than those in the PS network with $M \to \infty$. From the figure we can see that the topological interaction starts to affect the slow transport process of a molecule in the semidilute regime at relatively low values of $M/M_{e,PS} \simeq 0.1$, thus the free Rouse chain behavior being observed in a limited narrow range of c_{PS} and M. If we attempt to approximate the curve above $M/M_{e,PS} = 1$ by a straight line, we obtain 1.1 as its slope. This value gives the exponent of 2.1 for the MW dependence of f, which is slightly larger than the value of 2 predicted by the reptation theory.

Figure 9 gives the concentration dependence of $s(0.1M_{e,PS})$, being reciprocally proportional to the effective

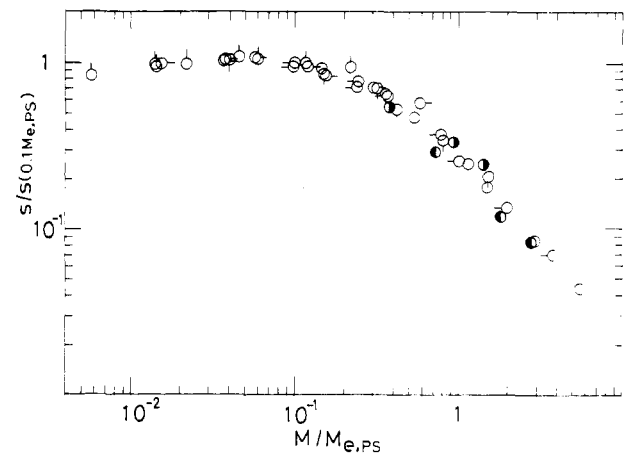

Figure 8. Master curve constructed from the s data in Figure 7 by the reduced plot of $s/s(0.1M_{e,PS})$ against $M/M_{e,PS}$. Symbols are the same as in Figure 7. The s data of the F80 series at c_{PS} = 10 and 16 wt % are also reduced and are shown in the figure. Symbols are (◑) c_{PS} = 10 and (◐) c_{PS} = 16 wt %.

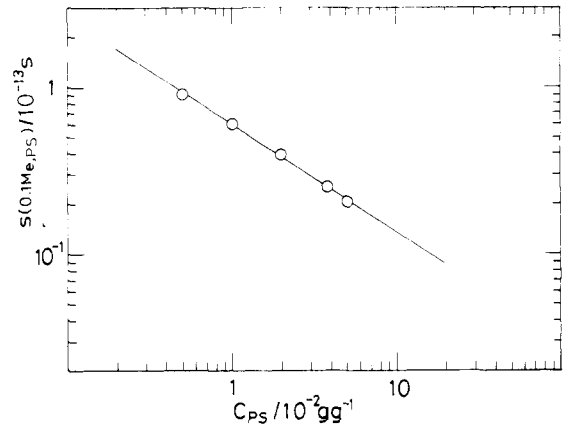

Figure 9. PS concentration dependence on $s(0.1M_{e,PS})$, which has been used for reduction of the s data in Figure 7.

Table IV
Values of A and δ Obtained from a Fit of Eq 10 to the Concentration Dependence of s

$M \times 10^{-4}$	in F4-TPh		in F80-TPh		in F840-TPh	
	A	δ	A	δ	A	δ
10.7			60	0.65	63	0.67
26.5	28	0.81	80	0.65	93	0.62
40.1			98	0.62	119	0.58
84.4			113	0.62	144	0.60
110			123	0.63	175	0.58
214	27	0.80	133	0.62	219	0.57
405					258	0.58

friction coefficient $\zeta(c_{PS})$. The data can be well represented by a straight line whose slope is $-(0.68 \pm 0.02)$. Theories have predicted that, for homogeneous solutions, ζ increases with increasing c as c^{γ} with an exponent varying from 0.5 in good solvents to 1 in the Θ state. The value 0.68 is intermediate between them.

In order to test our superposition procedure, s data of F80 series at c_{PS} = 10 and 16 wt % (the two bottom curves in Figure 3) have been reduced by calculating $M_{e,PS}$ with eq 13 and reading $s(0.1M_{e,PS})$ at respective c_{PS} from long extrapolation of the straight line in Figure 9. The reduced data, shown as half-filled circles in Figure 8, all come close to the master curve.[31] This suggests that local free volume correction on ζ may be small up to c_{PS} = 16 wt %,[25] giving additional support for our procedure.

It should be emphasized that superposition has been successfully achieved without any adjustable parameter. As a result, the topological function ψ has been uniquely determined as a function of $M/M_{e,PS}$. The knowledge of ψ and ζ in Figures 8 and 9 enables us to calculate s at any other c_{PS} and M without the help of theory. In part 5 of this series, s data in this work will be compared with the theoretical prediction by Hess[26] and also with existing D_s data in both semidilute regime and melts. From such a comparison, physical significance of the function ψ will be clarified. Why the use of $M_{e,PS}$, compared with other quantities such as the hydrodynamic screening length based on the blob model, is a better representation of effects of the hydrodynamic and the topological interaction on polymer dynamics will also be studied in part 5.

Finally it may be remarked that the concentration dependence of the F840 series s data for each molecular weight can be well described by eq 10 with A and δ values listed in Table IV and by the fact that all s/s_0 versus c_{PS} curves can be superposed on one other by horizontal shifting.

Acknowledgment. We are greatly indebted to Dr. T. Fukuda of this institute and Prof. T. Nose of Tokyo Institute of Technology for a gift of valuable PMMA samples and helpful discussion. This work was partly supported by a Grant-in-Aid from the Ministry of Education, Science and Culture, Japan (Grant 59470090).

Registry No. PMMA, 9011-14-7; PS, 9003-53-6.

References and Notes

(1) de Gennes, P.-G. *Scaling Concepts in Polymer Physics*; Cornell University Press: Ithaca, NY, 1979.
(2) Leger, L.; Hervet, H.; Rondelez, F. *Macromolecules* **1981**, *14*, 1732.
(3) Wesson, J. A.; Noh, I.; Kitano, T; Yu, H. *Macromolecules* **1984**, *17*, 782.
(4) Callaghan, P. T.; Pinder, D. N. *Macromolecules* **1984**, *17*, 431.
(5) Wheeler, L. M.; Lodge, T. M.; Hanley, B.; Tirrell, M. *Macromolecules* **1987**, *20*, 1120.
(6) Doi, M.; Edwards, S. F. *J. Chem. Soc., Faraday Trans. 2* **1978**, *74*, 1789.
(7) Klein, J. *Macromolecules* **1978**, *11*, 852.
(8) Daoud, M.; de Gennes, P.-G. *J. Polym. Sci., Polym. Phys. Ed.*. **1979**, *17*, 1971.
(9) Numasawa, N.; Kuwamoto, K.; Nose, T. *Macromolecules* **1986**, *19*, 2593.
(10) Freed, K. F.; Edwards, S. F. *J. Chem. Phys.* **1974**, *61*, 3626.
(11) de Gennes, P.-G. *Macromolecules* **1976**, *9*, 594.
(12) Kim, H.; Chang, T.; Yohanan, J. M.; Wang, L.; Yu, H. *Macromolecules* **1986**, *19*, 2737.
(13) Nemoto, N.; Inoue, T.; Tsunashima, Y.; Kurata, M. *Bull. Inst. Chem. Res., Kyoto Univ.* **1984**, *62*, 177.
(14) Nemoto, N; Inoue, T; Makita, Y; Tsunashima, Y; Kurata, M. *Macromolecules* **1985**, *18*, 2516.
(15) Fukuda, T.; Nagata, M.; Inagaki, H. *Macromolecules* **1984**, *17*, 548.
(16) The molecular weight of the sample P-1 was erroneously reported as 342 000 due to a simple mistake in calculation of the buoyancy term. M_w = 260 000 has been recalculated from D_0 and s_0 by using a correct value for the term.
(17) During this experiment, the molecular weight distribution of the highest molecular weight sample (P-400) was found to be a little bit broader than that of other anionically polymerized samples.
(18) It is not clear why the exponent for k_s is not attained to 0.8, the theoretical asymptotic value in the good-solvent limit.
(19) Osaki, M.; Nishizawa, K.; Kurata, M. *Macromolecules* **1982**, *15*, 1068.
(20) Yamakawa, H. *Modern Theory of Polymer Solutions*; Harper and Row: NY, 1971; Chapter VI.
(21) Akcasu, Z.; Benmouna, M.; Han, C. C. *Polymer* **1980**, *21*, 866.
(22) Sedimentation velocity measurements have been made on higher molecular weight samples of PMMA at c_{PS} = 10 and 16 wt %. Unfortunately, a peak of sedimentation pattern hardly moved down from the meniscus in spite of a 1-week run. Though it was possible to calculate s from such photographs, s values obtained are less reliable compared with other s data in Figure 3. Therefore we just disregarded those s values in this work.
(23) Phillies, G. D. J. *Macromolecules* **1986**, *19*, 2367.
(24) Marmonier, M. F.; Leger, L. *Phys. Rev. Lett.* **1985**, *55*, 1078.
(25) Nemoto, N.; Landry, M. R.; Noh, I.; Kitano, T.; Wesson, J. A.; Yu, H. *Macromolecules* **1985**, *18*, 308.
(26) Hess, W. *Macromolecules* **1986**, *19*, 1395.
(27) Cukier, R. I. *Macromolecules* **1984**, *17*, 252.
(28) Altenberger, A. R.; Tirrell, M. *J. Chem. Phys.* **1984**, *80*, 2208.
(29) This may be tested from R_G measurements of PMMA in PS–Tph solutions, but such a measurement on a low molecular weight PMMA failed to give a reliable value.
(30) Two solvents, aroclor and thiophenol, are both good to PS. Nevertheless viscoelastic measurements on PS–Tph solutions in the semidilute regime might give a c–M_s relation different from eq 13. If a different exponent value is used, the success of superposition will deteriorate. However, Dr. Osaki informed us that if g cm^{-3} is used as a unit of concentration, eq 13 may be applicable, to a good approximation, to our particular system.
(31) The reduced s data with $M > M_{PS}$ in the F80 series have deviated upward from the master curve.